Thermal Protection System Design of Aerocapture Systems for Uranus Orbiters

Jonathan Morgan*, Ethiraj Venkatapathy†, Matthew Gasch‡
NASA Ames Research Center, Moffett Field, CA, 94035

Joseph Williams§, Rohan G. Deshmukh*
Analytical Mechanics Associates, INC., Hampton, VA, 23666

Eli Shellabarger*, James B. Scoggins*, Andrew Gomez-Delrio*, and Soumyo Dutta¶
NASA Langley Research Center, Hampton, VA, 23681

The National Academies Planetary Science and Astrobiology Decadal Survey recently identified Uranus and Neptune - the Ice Giants - as the priority destinations for science[1]. A mission to Uranus, the highest priority destination due to proximity to Earth, is viable with existing launch vehicle providers during launch windows starting in 2031. However, a nominal interplanetary trajectory (between 12 and 15 years) would still necessitate more than half the initial launch mass in propellant to achieve orbital insertion[2]. Aerocapture, a method of orbital control that directs aerodynamic forces generated on a vehicle by the planet's atmosphere, allows mission designers to achieve the desired orbital state while saving time to the final destination and increasing the available mass for the science payload. Achieving orbital insertion via aerocapture requires novel algorithms for Guidance, Navigation and Control[3], and mass-efficient Thermal Protection Systems (TPS) performing in an atmosphere unlike any other NASA has flown through. Multiple TPS in NASA's repertoire are suitable for the unique aerothermal environment on the forebody, and the results of predicted sizing and challenges in implementation are discussed below. Results for aftbody TPS made by NASA as well as commercial vendors are discussed, along with the discussion of alternative solutions that may save time, reduce complexity, and increase mass-efficiency for the recommended Uranus Orbiter and Probe mission.

I. Nomenclature

q_{conv}	=	convective heat flux, W/cm^2
q_{rad}	=	radiative heat flux, W/cm^2
T	=	thickness, cm
ΔV	=	change in velocity, km/s
σ	=	standard deviation
μ	=	mean value

subscripts

1	=	nominal branch
2	=	aerothermal branch
3	=	material branch
RSS	=	Root-Sum-Squared result

*Aerospace Engineer, AIAA Member.
†Senior Technologist, AIAA Associate Fellow.
‡Senior Research Scientist, AIAA Member.
§Aerospace Engineer associated with NASA Ames Research Center, AIAA Member
¶Aerospace Engineer, AIAA Fellow.

II. Introduction

The National Academy of Sciences focused the next decade of scientific priorities on the outer planets Uranus and Neptune - the Ice Giants - because of their unique structure and place in our solar system. It is postulated that these bodies contain crucial information within their atmospheres, magnetospheres, and captured satellites essential for our understanding of solar system formation. Beyond that, the Ice Giants feature interesting characteristics such as the rings and Uranus's unique tilt and rotational direction which offer clues to the evolution of the solar system. In addition, Neptune's moon, Triton, could contain a subsurface ocean that harbors the right conditions and components to support life [1].

Given the scientific significance of these outer planetary bodies, undertaking a comprehensive mission is imperative to address these fundamental questions. In pursuit of this goal, mission architects have developed concepts that send scientific payloads to the Ice Giants in the form of an orbiter and probe. Under the classical fully-propulsive paradigm of vehicle delivery, the time to orbital insertion around Uranus is approximately 13 years, as was shown in the Uranus Orbiter and Probe (UOP) concept[1]. The significant amount of fuel required for this mission severely constrains the available payload for scientific instruments, thereby limiting the quantity and potentially even the quality of gathered data. Furthermore, propulsive solutions are not viable for arrival velocities greater than 12 km/s, limiting the trajectory space for mission planners[4].

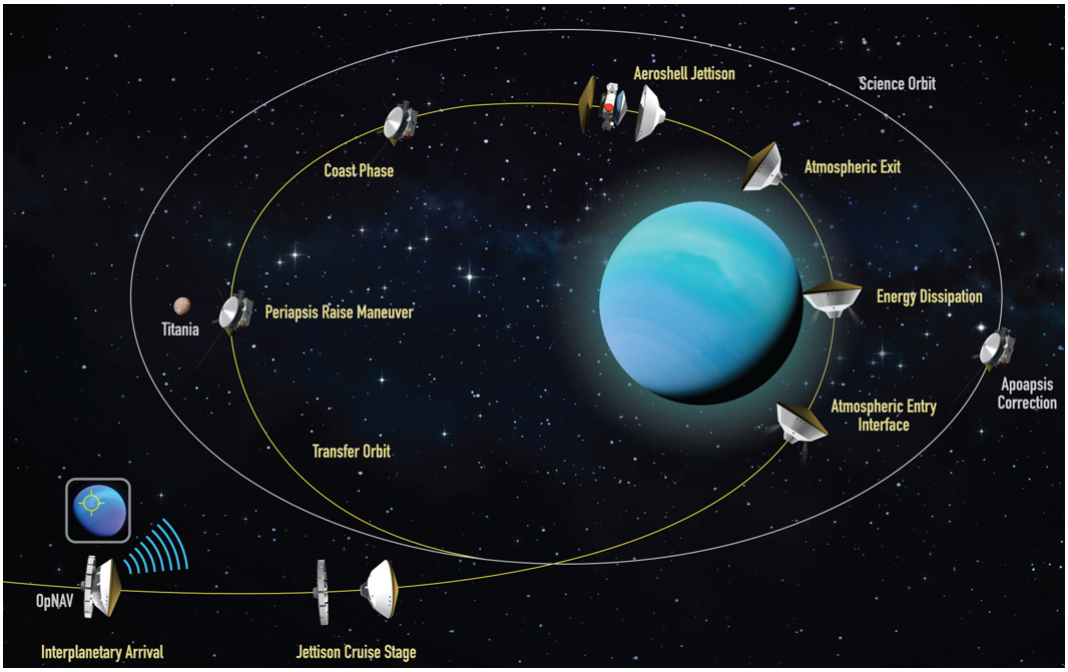

Fig. 1 Conceptual aerocapture approach to Uranus.

Aerocapture presents a promising alternative to propulsive orbital insertion by encasing the orbiter in an entry system, enabling navigation into and out of the planet's atmosphere to achieve a target orbit, shown conceptually in Fig.1. This orbital transfer maneuver can be accomplished in a variety of ways, most prominently by Bank Angle Modulation (BAM) as has been used for direct entry on Apollo, Mars Science Laboratory (MSL), Mars2020, and Orion, or by more sophisticated methods of Direct Force Control or Drag Modulated Aerocapture. Conceptual implementation of aerocapture has been studied at length for NASA applications[5–7]. The most recent investigations applied aerocapture as a method for orbital insertion to the Ice Giants by Dutta et al. [2] and Girija [4]. While mission studies to Venus, Mars, and even Titan consider heritage blunt body configurations, Ice Giants and their respective high-energy science orbits have in the past demanded new vehicle designs and/or thermal protection solutions. Designs of high lift-to-drag ratios (L/D 0.8) vehicles are novel in shape and would require considerable effort to validate aerodynamic performance, and at the time of the study, the predicted aerothermal conditions were greater than what existing TPS solutions could support. Work by Venkatapathy et al. [8], demonstrated conceptual solutions for more moderate L/D-ratio vehicles that construct aeroshells akin to heritage vehicles, but these designs still contain some asymmetric geometry and atypical heatshield configurations. Now, guidance, navigation, and control (GNC) schemes have demonstrated robust performance on much

lower L/D configurations such as heritage blunt body shapes even when considering current atmospheric uncertainties[3]. As Uranus is the highest-priority destination for the next decade, a detailed study evaluating the feasibility of delivering a scientific payload to Uranus's orbit using aerocapture is underway[9]. In the same study, specific works delve into mission design, GNC, aerodynamics, and aerothermodynamics and vehicle design considerations[10–14]. This paper focuses on the implementation and development of TPS for a traditional entry vehicle that applies bank-angle control to successfully achieve a specific scientific orbit via aerocapture. A brief overview of the concept of operations, the vehicle geometry, and the predicted aerothermal environments is presented in Section III. In Section IV the discussion moves to the TPS sizing process and uncertainties associated with determining the required thickness. Section V and Section VI contain analysis of the TPS trade-space for the forebody and backshell heatshields, and their implementation on the vehicles. Finally, conclusions and forward work for the study are discussed in Section VII.

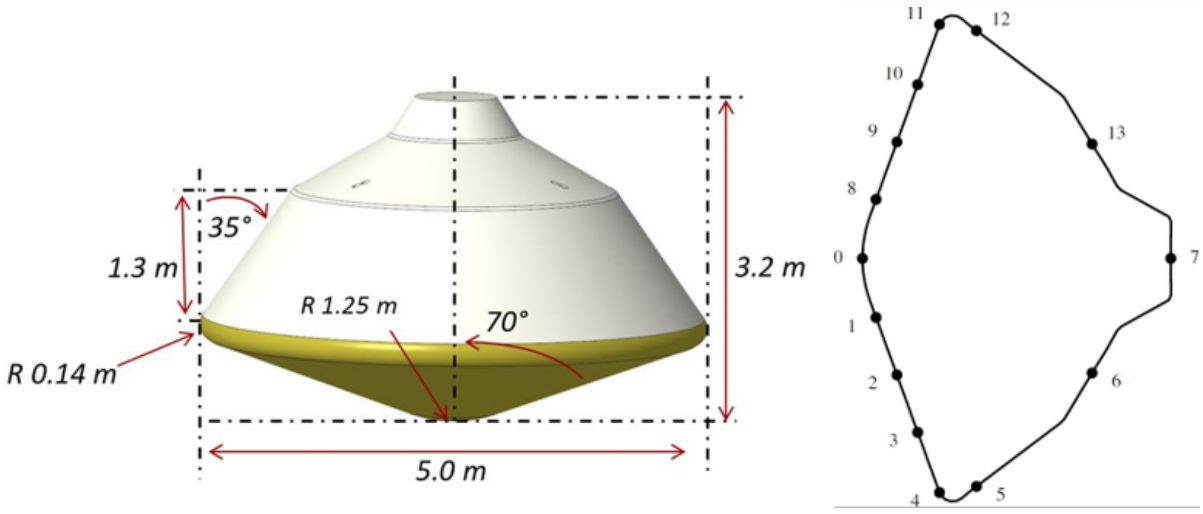

(a) Geometric definition of the concept aerocapture vehicle **(b) Body point (BP) mapping**

Fig. 2 (a) Scaled MSL geometry for the concept vehicle with dimensions given in and (b) vehicle body point mapping for analysis: points (1 - 6) are windward and points (8 - 13) are leeward.

III. Background

The geometry of the designed aerocapture vehicle chosen to deliver the science payload is a scaled version of the MSL entry vehicle. The 70° sphere cone forebody extends to an expanded diameter of 5 meters with a nose radius of 1.25 meters, shown in Fig.2. The vehicle has a 14 cm shoulder radius to interface with a 37° backshell similar in profile to the MSL vehicle. Bank Angle Modulation was chosen due to its relative simplicity in implementation and flight-proven execution for direct entry and rendezvous applications. Onboard instruments inform the BAM scheme as the vehicle navigates to the planet and through the atmosphere. The solution space for atmospheric navigation - the spacecraft entry corridor - is bounded by two trajectories, a maximum Lift-Down and a maximum Lift-Up trajectory. The Lift-Down trajectory represents the shallowest entry flight path angle, skimming the atmosphere thereby yielding the longest entry pulse with the lowest applied heating to the spacecraft. The Lift-Up trajectory is the opposite case with the steepest entry flight path angle that descends further into the atmosphere, achieving the necessary ΔV in less time at the cost of more severe entry environments on the spacecraft. These two stressing trajectories create unique analysis cases for evaluating aerothermal environments and required TPS thickness.

Uranus' atmosphere is made up of mostly Hydrogen and Helium with various other trace elements[15], most notably methane (CH4). Explored in Titan entry studies[16], methane is a strong radiator and can contribute to surface heating of the spacecraft, however, it is presently estimated to be confined to altitudes with impact at greater arrival velocities than the approximate 27 km/s in this aerocapture study. Heatshield release is planned within 10 minutes of atmospheric exit, defined as 1200 km geodetic altitude for TPS sizing purposes. This additional time where the heatshield is attached to the vehicle must be be captured in the sizing process to ensure that bondline temperatures are not exceeded as degraded TPS and substructure integrity could affect vehicle operations.

The nominal hot-wall, smooth surface entry environments for the Lift-Up and Lift-Down trajectory are generated from 3D CFD simulations using LAURA/HARA [12]. The 3D simulations are needed because the vehicle is oriented with a nominal angle of attack of 17°, shifting the stagnation point along the flank section instead of the nose cap, similar to the Mars2020 entry. The simulations predict laminar flow, though it is noted that transition to turbulence may be possible at some point along the leeward flank. Shown in Fig.3, the forebody environments differ from other missions in the long duration of the heat pulse, resulting in a high heat load laid out in Table 2 that the TPS must withstand. Even so, there exists minimal radiative heating and very low pressure and shear, owing to the low density of the upper atmosphere and gas species present. These unique environments pose an interesting case in TPS selection and analysis. The applied heating rates are significant enough to demand ablative thermal protection materials, but it is the heat load that is most extreme compared to most EDL missions, necessitating thicker solutions to insulate the spacecraft than may have been considered previously. Only the Galileo probe had comparable heat loads but at significantly greater heat fluxes which required the use of fully-densified carbon-phenolic (FDCP). FDCP is no longer manufactured and would be an incredibly heavy solution for this vehicle. Thankfully, more mass-efficient, mission enabling TPS technologies have been developed at NASA since Galileo that suit the predicted aerocapture environments. Figure 4 shows the nominal aftbody environments for selected body points on the Lift-Up trajectory. These environments also differ from typical missions by exhibiting low magnitudes in all commonly used indicators: pressure, shear, and total heat flux. The Lift-Down trajectory environments are not shown but are approximately 75% of the magnitude in all indicators. For each set of environments, the radiative heating is seen to abruptly drop due to a change in the fitting of data above and below specific speeds in the LAURA/HARA analysis. This has little impact as the radiative heating environment is small compared to the convective heating.

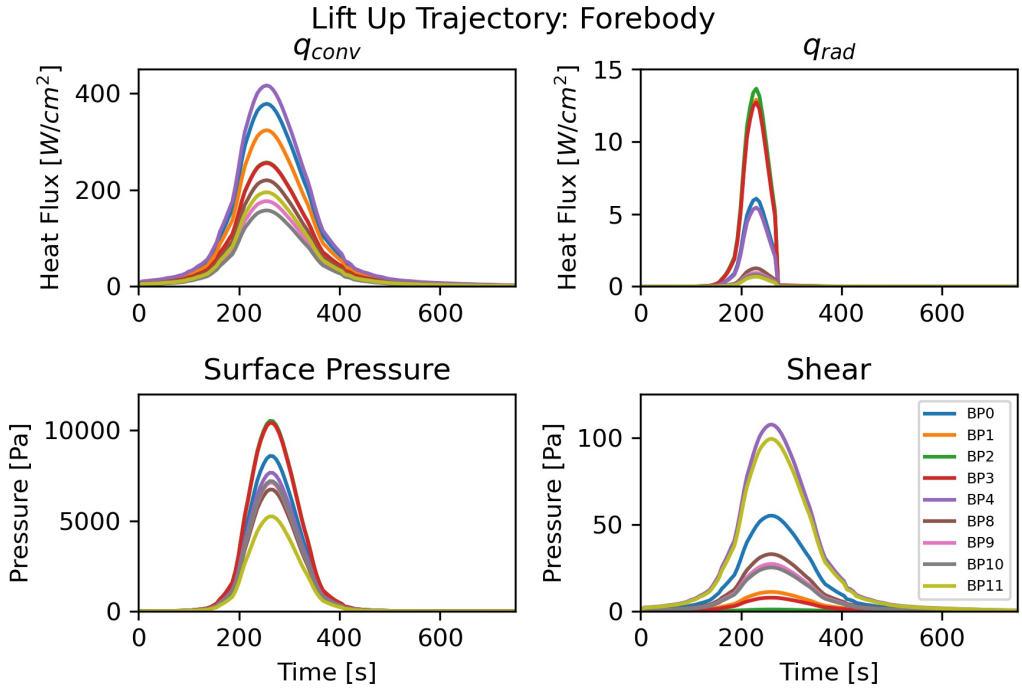

(a) Lift-Up

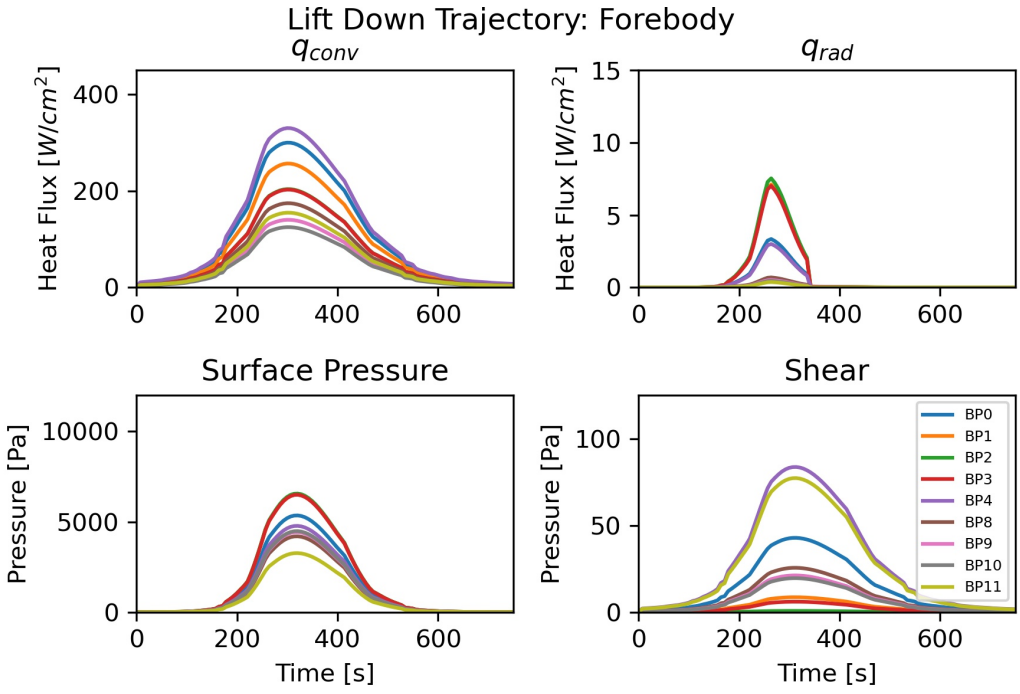

(b) Lift-Down

Fig. 3 Forebody environment predictions for each trajectory on select body points.

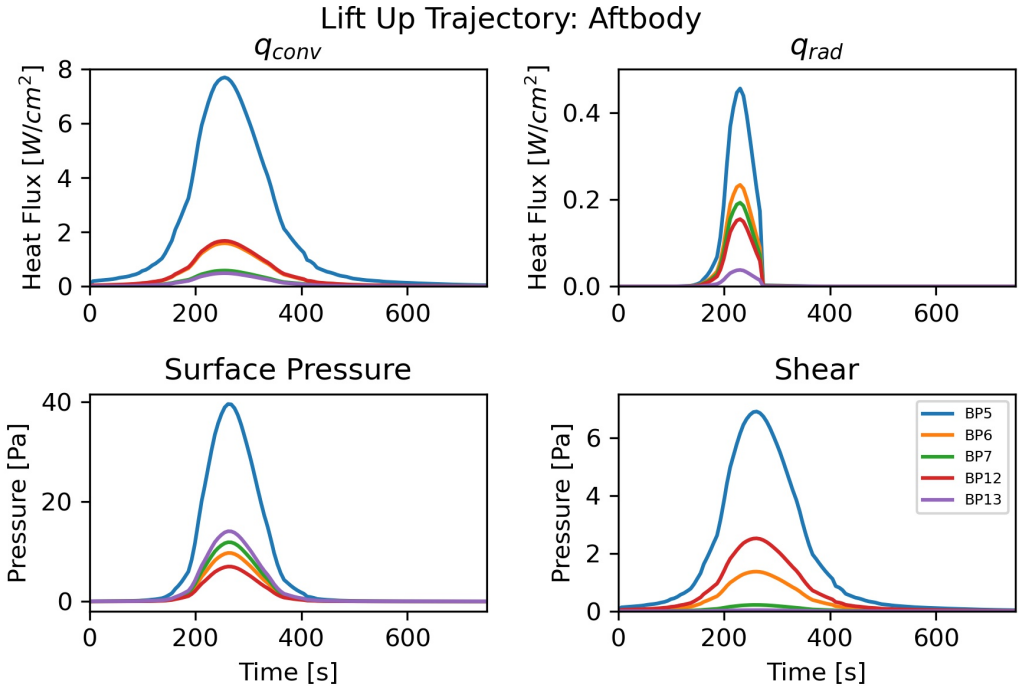

Fig. 4 Aftbody environment predictions for the Lift-Up trajectory on select body points.

BP	0	1	2	3	4	8	9	10	11
Lift-Up	66	56	44	44	72	38	30	27	34
Lift-Down	79	68	54	53	87	46	37	33	41

Table 2 Total heat load (kJ/cm^2) of the Lift-Up and Lift-Down tajectory on each forebody body point.

IV. Sizing Methodology

Determining the appropriate TPS thickness given a mission's design trajectories and environments carries important implications for material selection and ultimately mission feasibility. TPS material thickness optimization is driven by constraints on substructure operating temperatures. These constraints are applied until a time specified by mission designers, typically the time when the hardware has completed its primary function, such as heatshield or backshell release. The optimized thickness then enters a margins policy to account for material and environmental uncertainties. This margin policy, in conjunction with the assumptions and constraints in the optimization phase, constitutes the sizing methodology. TPS sizing must strike a balance in adequately enveloping the uncertainties in trajectory, aerothermal environments, and material response, while also avoiding overly conservative solutions which add unnecessary mass to the spacecraft.

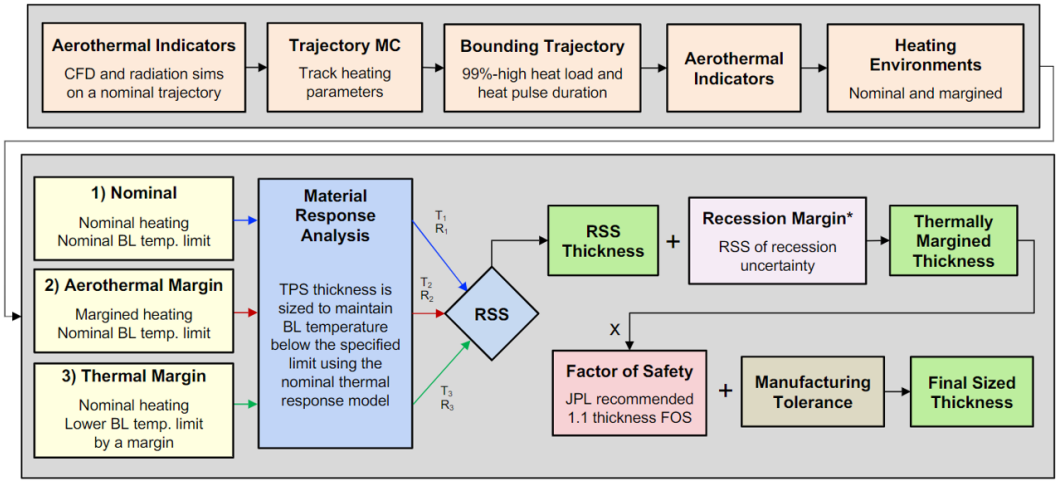

Fig. 5 Three-branch TPS sizing approach used for Mars2020.

Figure 5 illustrates the sizing process used for Mars 2020 in a simplified diagram. This process is largely derived from the TPS sizing methodology developed by the MSL and Orion teams and was successfully used for those missions[17]. Key body points, such as the nose cap, stagnation point, and shoulder are separately evaluated in this methodology. This allows for tuning of body point specific details like surface curvature or substructure definition. For Uranus aerocapture, the Lift-Up and Lift-Down design trajectories and environments discussed in the previous section are the nominal branch inputs. Next, each body point is sized in two other branches that account for independent sources of uncertainty. The aerothermal branch covers uncertainty in the aerothermal environments. Input multipliers for the convective heating, radiative heating, and pressure quantify the cumulative uncertainty. The thermal branch adds conservativism associated with material property uncertainty. It is quantified as a substructure temperature constraint margin. For the Uranus aerocapture study, the temperature margin is applied to the TPS-adhesive interface. This bondline temperature margin is the product of a Monte Carlo analysis conducted at the thickness driving body point and trajectory determined by the nominal branch. Within the Monte Carlo analysis, material property perturbations are informed by $2\sigma/\mu$ gaussian distributions. Besides material properties, all other analysis inputs are sourced from the nominal branch, including the TPS thickness. The sized thicknesses from these three independent branches are combined in a Root-Sum-Squared (RSS) formula, shown below in Eq.1.

$$T_{RSS} = T_1 + \sqrt{(T_2 - T_1)^2 + (T_3 - T_1)^2} \tag{1}$$

After the RSS calculation, various margins are stacked. In Mars 2020, a recession margin was added to account for the uncertainties in surface ablation modeling and a mismatch with some ground experiments. This process produces the thermally margined thickness, which may be multiplied by a mission-recommended Factor of Safety (FOS) followed by the addition of a manufacturing tolerance to arrive at the final sized thickness for a specific TPS subsystem, as had been done for Mars2020. This represents one scenario of stacked margins defined by material selection, modeling accuracy, and mission policy. The thickness attained after stacking margins, is the minimum design thickness for the analyzed body points.

Compared to the Mars 2020 sizing methodology, the Uranus aerocapture policy prescribes a few key differences. The non-oxidative Uranian atmosphere results in minimal recession. In fact, the only shape change realized is due to oxidative gases generated during material decomposition and through shrinkage of charred material. The consequence is no recession margin in the sizing process. Tiled heatshields commonly employ a gap filler margin, often 25%), to account for differential recession between the main TPS material and gap filler which can cause fencing or tunneling. Because there is minimal recession expected, there is no substantive differential recession and therefore no associated required margin. Secondly, factors of safety beyond those incorporated in the RSS process are viewed to be overly conservative and not used in most missions including this study. Thirdly, manufacturing tolerance are considered by the manufacturing team and not included in the aerocapture sizing methodology. This results in the exclusion of any stacked margin in the Uranus aerocapture sizing methodology. Lastly, the aerothermal margin approach is borrowed from an earlier study incorporating uncertainty in both the convective heating and the pressure measurements[18]. The aerothermal convective heating margin is chosen to be 35%, the radiative heating margin is chosen to be 50%, and the pressure margin is chosen to be a typical uncertainty of 5%.

V. Forebody Thermal Protection Systems

A. Candidate TPS

Four candidate TPS systems are considered for the forebody heatshield. Each is an ablative technology using material decomposition and low thermal conductivity to protect the vehicle during the aerocapture atmospheric maneuvers. These systems can be categorized by density, first looking at mid-density HEEET and 3MDCP, and finally low density PICA-D and C-PICA.

Previous studies dedicated to the outer solar system have conveyed the need for TPS capable of performing at heat fluxes exceeding 1000 W/cm^2 while at pressures greater than 100 kPa. NASA developed the Heatshield for Extreme Entry Environment Technology (HEEET) material as a replacement for the heritage capability of FDCP and to protect vehicles with entry environments in the kilo-watt range with large dynamic pressures. The HEEET system is a technology that integrally weaves together two layers of woven TPS that are optimized for recession and insulation. The first layer is a dense, carbon-rich (HEEET-RL) outer layer optimized for recession at the target environment. The second layer is a phenolic-rich insulative (HEEET-IL) layer sized to keep the underlying bondline temperature below a target limit. At reduced pressures and heat fluxes, such as those predicted for this mission, a mass savings option allows for use of only the insulative layer of this system as an ablator. The concept of using only the insulative layer has already been carried forward and exists today as 3D Medium Density Carbon Phenolic (3MDCP). A single-piece 3MDCP heatshield is planned for the Earth Entry System (EES) as part of the Mars Sample Return (MSR) project. 3MDCP has not been developed with a gap-filler in mind at the time of writing, and one would be needed for the aerocapture vehicle as the single-piece weaving architecture for MSR-EES only supports a 1.3 meter vehicle.

The Phenolic Impregnated Carbon Ablator (PICA) has flown as the forebody TPS for Stardust, MSL, Mars2020, and Osiris-Rex. PICA heatshields are manufactured in either a single-piece or tiled configuration with Room Temperature Vulcanizing silicone (RTV-560) as a gap-filler depending on the vehicle size. The system is made from a rigid carbon substrate called Fiberform that is then infused with low-density phenolic resin. Environments previously experienced by PICA for flight missions are both significant and relevant to the Uranus aerocapture. In addition, an extensive ground test history in the arc jets exceeds anticipated aerocapture mission environments, reducing risk in implementation. PICA-D is the modern version of heritage PICA using similar manufacturing processes and materials.

Relatively new to the family of TPS developed by NASA is Conformal PICA (CPICA) which represents an important improvement to TPS - flexibility. CPICA is made from carbonized felt possessing lower through-thickness conductivity than FiberForm, that is then infused with low-density phenolic resin. The felt may either be carbonized to a custom shape, or the final infused part may bonded to a curved surface as the felt has a higher strain to failure than PICA-D. Conforming to the outer mold line of the spacecraft is desirable thermally, too, as the material is minimally conductive

when the felt fibers are perpendicular to the vehicle surface normal. This flexibility is most important at the vehicle shoulder where previous incarnations of PICA tiles have exposed side faces to the entry environment, resulting in significant energy transfer, reducing the efficiency of the TPS. CPICA has not yet flown as a forebody or backshell TPS, but the performance has been demonstrated in arc jets with gap-filler concepts similar to those executed in Mars2020.

B. Results

The forebody TPS sizing incorporated elements of the system design as well as aerothermal predictions to simulate the TPS thermal response during atmospheric entry. These elements are presented below along with the resultant TPS thicknesses. The material selection in the forebody substructure stack-up largely reflects the stack-up used to construct the Mars 2020 aeroshell. However, substructure material thicknesses are kept uniform instead of the variable ply thicknesses and densities used for the Mars2020 vehicle. The substructure materials and corresponding thicknesses are shown in Table 3. HT-424 is a commonly used TPS adhesive with flight heritage from human spaceflight dating to the Apollo entry systems to sample return missions such as Stardust. Below the HT-424 adhesive, 60mm thick, 2.1 lb/ft^3 dense aluminum honeycomb is sandwiched between thin M55J graphite fiber facesheets.

Material Selection	Material Thickness [cm]
HT-424	0.025
M55JA composite	0.1
Al-hc-21.-2.5in	6.0
M55JB composite	0.1

Table 3 Forebody substructure definition.

The adhesive choice is the limiting temperature constraint in this system, restricting the maximum bondline temperature to 250 $°C$ and ultimately driving the TPS thickness during sizing optimization. The 250 $°C$ peak bondline temperature is equivalent to the rated short term operating temperature of HT-424 per manufacturing guidelines. Another key decision in the sizing problem formulation is the initial temperature of the stack-up just prior to Uranus atmospheric entry. The solar energy at Uranian distances is relatively low and internal heating systems are unlikely to keep the large heatshield warm but to hold a healthy temperature margin, the initial temperature is biased warm and assumed to be -10°C. The freestream temperature for radiating was averaged over the trajectory and a single 10 °C constant was implemented. With the problem framed, sizing began according to the methodology laid out in Section IV. Simulations were performed using the Fully Implicit Ablation and Thermal response program (FIAT) which computes transient one-dimensional thermal response and surface thermochemistry of TPS stack-ups and is used in design optimization. Nominal branch thickness solutions for each forebody body point and candidate TPS system are shown in Table 4. Material systems are presented in order of increasing thermal conductivity.

[cm]	C-PICA		PICA D		3MDCP	
BP	Lift Down	Lift Up	Lift Down	Lift Up	Lift Down	Lift Up
0	3.58	3.12	6.31	5.46	4.50	3.88
1	3.39	2.94	5.92	5.10	4.19	3.61
2	3.19	2.77	5.58	4.79	3.83	3.30
3	3.19	2.76	5.57	4.78	3.83	3.30
4	3.57	3.11	6.24	5.40	4.56	3.94
8	3.02	2.61	5.30	4.53	3.58	3.08
9	2.84	2.44	4.97	4.24	3.27	2.81
10	2.74	2.36	4.80	4.09	3.12	2.67
11	2.90	2.50	5.10	4.35	3.40	2.92

Table 4 Nominal TPS thickness for CPICA, PICA-D, and 3MDCP for each trajectory on all forebody body points.

A few trends exist across the material systems. The Lift-Down trajectory drives the largest thicknesses due to the higher heat load. Windward body points all require more material than any leeward location owing to both more stressing heat rates and heat loads. Finally, body points 0 and 4, representing the vehicle nose and windward shoulder respectively, are the most demanding TPS locations in thickness. Interestingly, the lower conductivity PICA-D system requires more thickness than the higher conductivity, mid-density 3MDCP system. This result is likely tied to the amount of material decomposition impacting the TPS blowing into the boundary layer and reducing effective heating. Table 5 shows areal mass loss across the Lift-Down trajectory at body point 4 with 3MDCP generating three times more decomposition products over the aerocapture maneuver.

CPICA	PICA-D	3MDCP
1.67	1.59	4.91

Table 5 Shoulder (body point 4) TPS areal mass loss (kg/m^2)**.**

Monte Carlo analysis was performed for each material system at body point 4, generating a thermal margin and informing the third branch of sizing in the RSS process. Material property 2 σ/μ uncertainties were adopted from the Mars 2020 project. These uncertainties were applied to virgin and char TPS terms like density, specific heat, conductivity, and emissivity. Each substrate material system received uncertainties for a similar list of virgin properties. A few additional terms were perturbed in the TPS: decomposition parameters, blowing reduction, and pyrolysis gas enthalpy. For this study, all forebody TPS candidates were treated with the same uncertainties presented in Table 6. This assumption is likely fair for CPICA and PICA-D however, 3MDCP is different enough that future refinements should consider using tailored uncertainties. Indications from 3MDCP development is that the applied uncertainties are conservative.

TPS Parameter	$\frac{2\sigma}{\mu}$ Uncertainty	Substrate Parameter	$\frac{2\sigma}{\mu}$ Uncertainty
TPS Virgin State		Adhesive	
Density	5	Density	10
Specific Heat	5	Specific Heat	10
Conductivity	20	Conductivity	20
Emissivity	5	Thicknes	25
TPS Char State		Honeycomb	
Density	same as Virgin	Density	5
Specific Heat	10	Specific Heat	10
Conductivity	same as Virgin	Conductivity	25
Emissivity	5	Thickness	5
Other		Facesheet	
Decomposition Parameter	20	Density	10
Blowing Reduction	20	Specific Heat	10
Pyrolysis Gas Enthalpy	25	Conductivity	25
		Thickness	10

Table 6 Uncertainty in material modeling parameters for Monte Carlo simulations.

The binned results of the maximum bondline temperature from 10,000 Monte Carlo runs are shown in Fig.6 for each material system. Based on the given environment and TPS thickness, a mean maximum bondline temperature equivalent to the nominal branch optimization constraint, 250 $^{\circ}C$, is expected. The thermal margin is equal to the one sided, 3σ value reduced by the mean. This thermal margin is then used as a knockdown in the bondline temperature constraint to size this branch. The Monte Carlo analysis generally converged within 2,000 runs and the TPS thermal

conductivity, both virgin and char, were the most correlated to the peak bondline temperature.

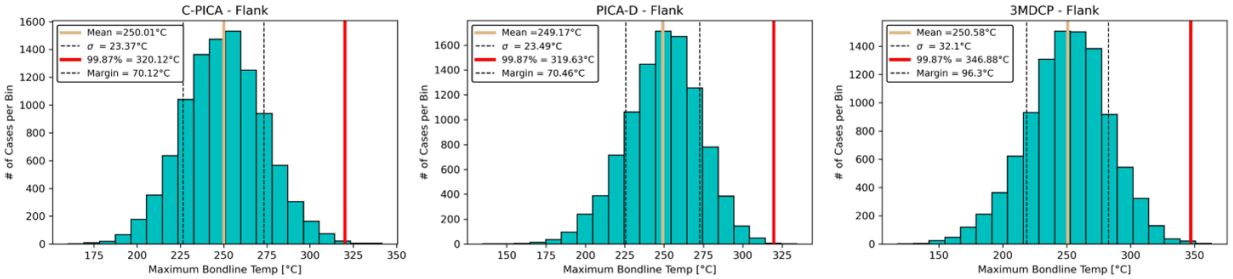

Fig. 6 Monte Carlo results and thermal margin.

Finally, through incorporating each of the three branches, the results of the RSS thicknesses are presented in Table 7. Observed trends follow those discussed from the nominal branch. Evaluating the thickness-driving Lift-Down trajectory, thickness variation by body point ranges from approximately 15% to 20%. This offers some mass savings benefits to varying TPS thickness by location on the forebody, especially since the variation mostly comes from the windward / leeward split. Caution needs to be given to future substructure definition changes, particularly to introduced variation by body point location. At this early junction, TPS thickness is assumed constant across the heatshield and asymmetric builds are noted as potentially viable.

[cm]	C-PICA		PICA D		3MDCP	
BP	Lift Down	Lift Up	Lift Down	Lift Up	Lift Down	Lift Up
0	5.22	4.61	8.70	7.81	6.47	5.80
1	4.97	4.36	8.32	7.42	6.16	5.51
2	4.71	4.12	7.99	7.10	5.81	5.19
3	4.71	4.11	7.99	7.09	5.80	5.18
4	5.17	4.57	8.59	7.72	6.50	5.84
8	4.48	3.90	7.72	6.81	5.54	4.94
9	4.24	3.69	7.37	6.45	5.21	4.63
10	4.12	3.58	7.18	6.25	5.04	4.47
11	4.32	3.76	7.51	6.60	5.35	4.77

Table 7 RSS-sized TPS thickness for CPICA, PICA-D, and 3MDCP for each trajectory on all forebody body points.

Assuming a uniform thickness heatshield, TPS system mass efficiency is measured by areal mass which balances the sized thickness and material density of each system. Each approximate areal mass is tabulated below in Table 8. Lower areal masses translate to high mass efficiencies. CPICA is the desirable TPS material system for this Uranus aerocapture mission.

TPS	CPICA	PICA-D	3MDCP
Areal Mass kg/m^2	14	24	48

Table 8 Resultant Areal mass for each system from RSS-sizing.

A potentially important parameter, depending on the vehicle design and trajectory, is the time of heatshield separation. As mentioned in Section III, the current assumption is to release the heatshield at 10 minutes after atmospheric exit. Evaluating the bondline temperature history in each sizing branch for the given design trajectories provides insight into the importance of this parameter. In the current iteration of the study, the nominal and aerothermal branches shown in Fig.7 to reach the intended peak bondline temperatures less than 5 minutes after exit from the atmosphere. The result is that the first two branches are insensitive to any separation time greater than approximately 5 minutes and the third

branch is the only one impacted. This relative insensitivity is observed in sizing when separation is adjusted ±5 minutes from the nominal 10 minutes. Releasing 5 minutes earlier reduces the sized CPICA thickness by 2% while delaying by 5 minutes increases the thickness by 0.5%. While heatshield separation is not an important factor in the current design, previous design cycles have had a sensitivity on the order of 8% for the same time delta. Therefore, separation timing may offer mass penalty or savings in future designs and should be tracked.

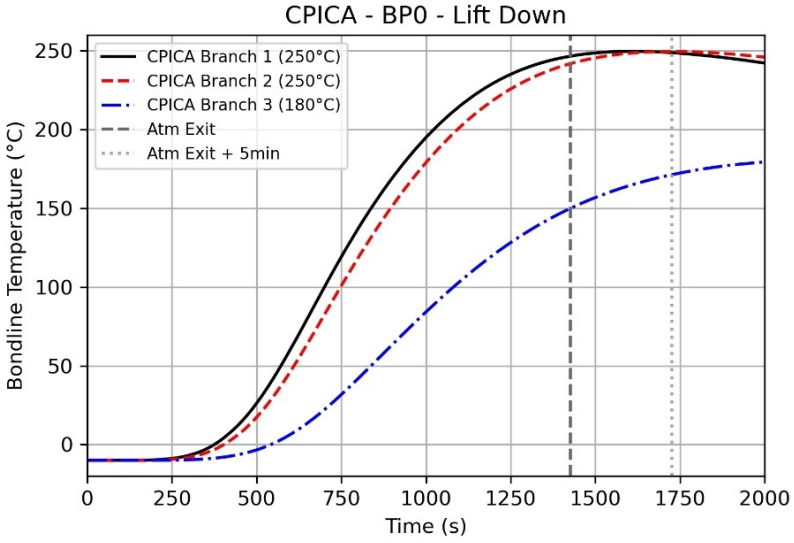

Fig. 7 Bondline temperature history for three-branch sizing

C. Testing

Ground testing in arc jets is a cheaper alternative to flight testing that allows TPS designers to investigate specific performance and failure characteristics of material systems in relevant environments. Key benefits when working within the PICA family is not only its succesful flight heritage, but the vast ground test history from development in the Orion, MSL, and Mars2020 programs as well as the capability sustainment efforts for PICA-D. Coupon-level testing for both PICA-D and CPICA in air exceed the predicted flight environments and do not exhibit failure for test points relevant to the flight envelope. More important, however, is Uranian atmosphere relevant test data in non-oxidizing environments, and testing PICA-D as a system with gap-fillers that would exist for the tiled heatshield. Figure 8 shows the PICA family test history in their respective test gas as a system with RTV-560 against the nominal and margined Lift-Up and Lift-Down trajectories discussed in Section IV. While this data set is not bounding, the test history is relevant and achieves heating levels that will engage material ablation mechanisms expected in flight, all while at an over-test in pressure - often a necessary by-product of achieving the target heat fluxes in arc jets. PICA-D models with a gap-filler model have eclipsed 280 W/cm^2 with 40 kPa surface pressure in non-oxidizing environments. As stated before, the non-oxidizing environments at moderate heat flux levels (below the sublimation limit for carbon) produce little in the way of recession. Of more concern, is the gap-filler performance where, under elevated temperatures, material degradation leaves behind a char that could allow hot gas to infiltrate and augment heating to the bondline. However, examination of post-test PICA-D models with RTV-560 gap-filler shown in Fig.9 exhibits no augmentation in the char layer depth. No models with CPICA and gap-filler have been tested in non-oxidative environments yet. Still, testing in air, which results in significant recession of the models, potentially exacerbating differential recession of the TPS material and gap-filler, did not uncover failures of the system for any one of the candidate gap-filler styles [19]. Testing CPICA with a relevant gap-filler in non-oxidizing environments would produce data that provides insight into performance of both components for a Uranus mission.

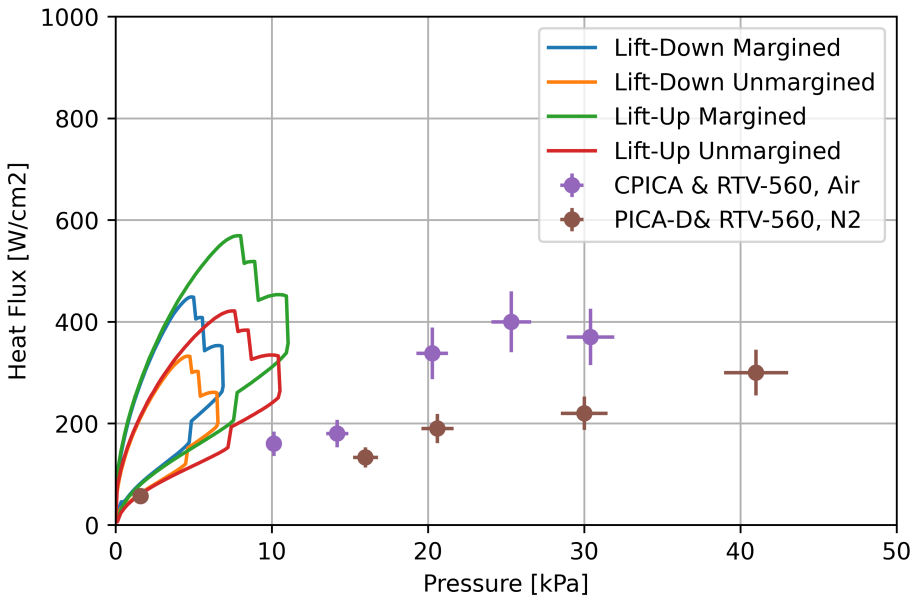

Fig. 8 Test history of PICA-D & RTV-560 in nitrogen and CPICA & RTV-560 in air compared to the aerothermal margined and nominal predicted environments of the Lift-Up and Lift-Down Uranus aerocapture trajectories. Typical heat flux uncertainties of 15% and pressure uncertainties of 5% are applied to the test data.

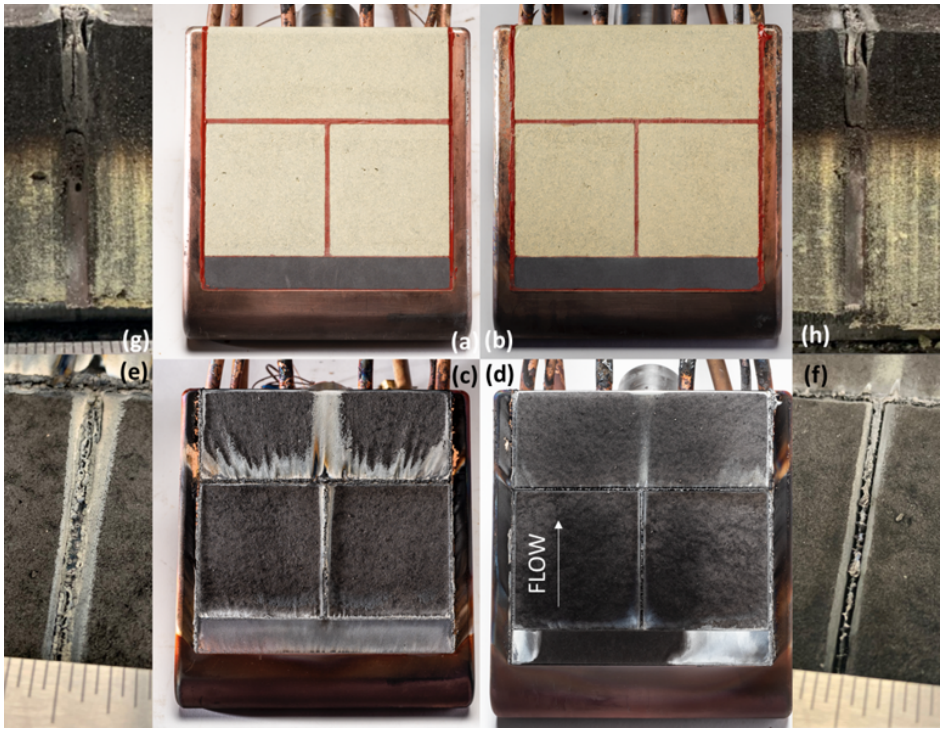

Fig. 9 Pictures of PICA-D & RTV-560 wedge models along with cross-section images. The model tested at approximately 140 W/cm^2, 16 kPa (a,c) has detail surface image (e) and cross-section (g). The model run at approximately 189 W/cm^2, 20 kPa is shown in (b,d) with detail and cross-section in (f,h) respectively.

D. Scaling and Manufacturing

Today's state of the art in ablative TPS offers no capability to manufacture a single-piece TPS for a 5 meter aeroshell. Therefore, producing a fully protected aeroshell requires use of tiled arrays of TPS material, as have large aeroshells in the past. PICA tiles for MSL and Mars2020 were infused as a block, cut to the necessary dimensions, and arranged intentionally to address three concerns: 1) the stagnation point of the flow must have minimal contact with the gap-filler, 2) the strike angle of the in-plane grain of PICA must be kept below 20°, and 3) the heatshield must limit the distance over which flow can travel parallel to a seam to match distances produced in ground testing[20]. This resulted in a tiled array shown in Fig.10.

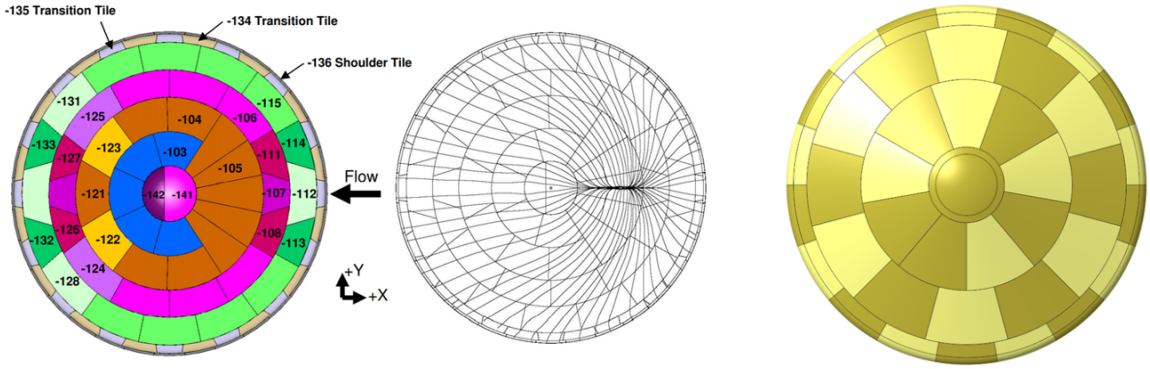

(a) MSL tile array of PICA informed by flowfield and PICA block size

(b) Conceptual tile array of CPICA

Fig. 10 Comparison of tile array for the forebody heatshield between MSL and the Uranus aerocapture vehicle.

CPICA is manufacturable as an infused block to much larger dimensions than PICA-D, 1.3 m square compared to $0.6mx$ 1.06 m. With an investment in tailored tooling for the vehicle, CPICA may be infused as a block with geometry to match the substructure. These two differences would simplify the number of gaps that must be filled and would reduce the overall machining required to integrate CPICA with the substructure. However, as was the case for MSL, testing may inform the longest streamwise parallel running length of a seam, see concern #3. Even without the potential benefit of larger tiles and few seams, CPICA can be infused in a molded shape, minimizing the strike angle of the in-plane grain with respect to the horizontal plane . Additionally, molding CPICA can ensure that the thru-thickness material orientation is parallel to the surface normal around the shoulder. Shown in Fig. 11, CPICA has been manufactured as a formed, $5cm$ thick part to a radius of curvature equal to $10cm$ which is smaller and more difficult to achieve than the shoulder radius of 14 cm for the conceptual forebody heatshield. There are several manufacturing implications of a formed shoulder, two large ones are: fewer individual tiles on the heatshield and a reduction in manufactured tile thickness to achieve as-designed tile thickness. While custom tooling is needed, and at complete scale-up in the CPICA manufacturing capability is needed to support a vehicle of this size, the benefits exhibited by the flexible TPS would reduce the overhead in machining so many pieces and reduce residual performance deficiencies faced by the PICA and RTV-560 system of previous missions.

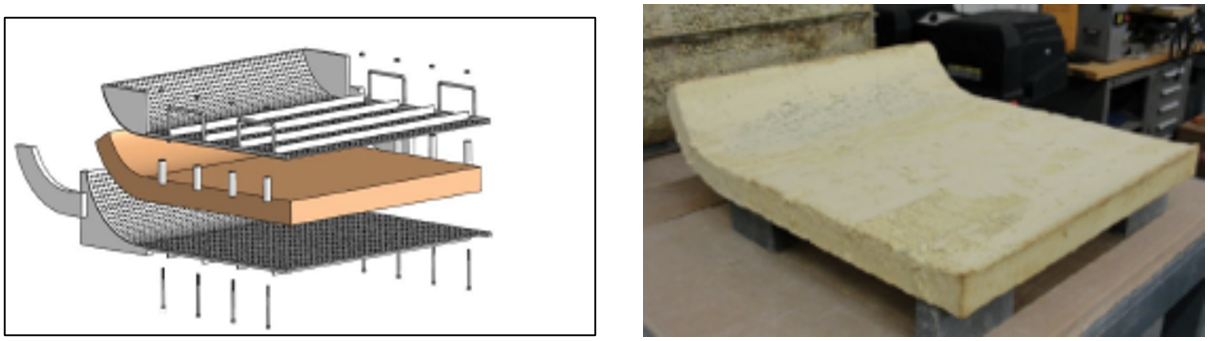

(a) exploded view of infused tooling design to support curved features

(b) Infused CPICA with curvature radius of approximately 10cm

Fig. 11 CPICA curved infusion demonstration

VI. Aftbody Thermal Protection Systems

The spacecraft's backshell geometry is shaped with two primary considerations: 1) to house the large antenna necessary for communications in deep space and 2) to keep intense forebody shocks and environments from impinging on the aftbody. The initial backshell design is inspired by the MSL backshell. Reaction control systems (RCS) thrusters are currently modeled, but future iterations may incorporate ports for navigation equipment needed to direct the spacecraft. The existence of such features may necessitate a tailored design beyond a single TPS like for MSL and Mars2020. Unique aftbody design aspects to consider are as follows: 1) RF-transparency for communications, 2) withstanding heating augmentation from RCS thruster operation, and 3) adequate heat rejection from the radiothermal generators housed within the aeroshell. However, as noted in Section III, the environments for the backshell are extremely benign, even when designing around higher entry velocities[12]. This allows for a broad consideration of many TPS materials and implementation types to meet the needs of the aftbody design.

A. Candidate Systems

The design space for backshell heatshields spans a considerable number of options. All typical backshell TPS options, from AETB-8 tile used on the Orion spacecraft to Lockheed Martin's Super Lightweight Ablator (SLA) 561-V which has significant flight heritage are applicable. However, it is important to consider the need for mass efficiency particularly with the scale of the backshell. Alternative systems with less flight heritage are also promising, like spray-on TPS, intumescent coatings, fabrics, or other flexible TPS. No material response model exists in FIAT for flexible protection systems like Nextel or Flexible SIRCA, or even for tested intumescent coatings like RX 2390, but arcjet results shows favorable performance for both NASA-made Flexible ablators and with FireX RX 2390, as described in Laub and White [21]. Spray-on TPS may hold the most promise for such a large backshell due to the ability to cover large areas in a single operation, but at present, the only coating known to the authors is Lockheed Martin's sprayable SLA-561S. To be adequately prepared for mission design, TPS solutions that can be installed with ease on a large and complex backshell stand to have a significant advantage in the trade space. An initial design sweep of common TPS for backshell purposes has been performed using Acusil-II, SLA-561V, and SIRCA-15. Many of these options have some capability as an ablative TPS and as such, are not optimized to be insulators for the extremely low environments predicted for the backshell.

B. Tailored Sizing for the Aftbody

TPS sizing for the backshell follows the forebody sizing process described in Section IV, with minor adjustments. As informed by previous missions like MSL and Mars2020, where the radiation contribution to backshell heating was found to be higher during flight reconstruction efforts, a significant margin is applied to the radiative heating portion, safeguarding against unknowns and non-conservative aerothermal predictions. In addition, owing to the possibly complex flowfield on the backshell, a 200% uncertainty in both the convective and radiative heating portions are applied in the aerothermal branch.

C. Results

Backshell entry environments can vary widely as shown in Fig.4. The substructure too can vary widely to satisfy design constraints in load, vehicle balance, communication, etc. The TPS backshell analysis is simplified to use the same substructure at all body points. The stackup is similar to the stack-up for the forebody shown in Table 3, but exchanges the honeycomb core variant for 0.75 inches of 4.3 lb/ft^3 density, and facesheets are half of the thickness of the forebody facesheet thickness. The process used in the forebody results section is again conducted for three backshell candidates. The nominal results are shown below in Table 9. The body points which experience the least heating, body point 7 on the closeout cone and body point 13 near the leeward shoulder, design bondline temperatures are not achieved when using any manufacturable thickness of any of the TPS. As expected, the windward shoulder point drives sizing due to the relatively large heating conditions.

Monte Carlo simulations performed on the aftbody material systems are shown in Fig.12 using adopted uncertainties from the Mars 2020 program. SLA values were used for SIRCA. Generally the material property uncertainties were lower in these systems and combined with the far more mild conditions resulted in significantly lower thermal margins.

[cm]	Acusil		Sirca		SLA	
BP	Lift Down	Lift Up	Lift Down	Lift Up	Lift Down	Lift Up
5	1.20	0.98	0.99	0.80	0.75	0.60
6	0.26	0.22	0.43	0.33	0.20	0.17
7	BLT Not Reached		BLT Not Reached		BLT Not Reached	
12	0.28	0.24	0.45	0.35	0.22	0.18
13	BLT Not Reached		BLT Not Reached		BLT Not Reached	

Table 9 Nominal branch results for aftbody sizing for each trajectory on each body point.

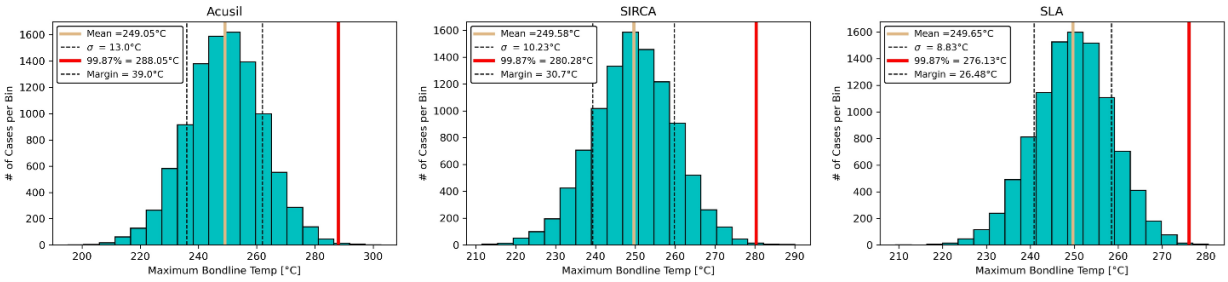

Fig. 12 Monte Carlo simulation results for three candidate backshell TPS.

Final sized thicknesses were calculated by completing the RSS sizing methodology and are shown in Table 10. The Lift-Down trajectory requires the most protection, again due to heat load. All three material systems are in the same density range, although SLA-561V is slightly lower making it the optimal choice among these options, when ignoring other requirements such as RF transparency.

In the work of Gomez-Delrio and Dutta [14], it is seen that there is margin in the position of the center-of-gravity. Vehicle designers may choose to keep the thick TPS as a ballast, but must again be wary of the need to reject heat from the generators housed within, and cognizant of the mass-growth that vehicles experience during the design and manufacture phase.

D. Scaling and Manufacturing

The traditional TPS like SLA-561V, SIRCA-15, and Acusil-II can adequately perform in the predicted environments but need to be thick in order to maintain the bondline temperature constraint over such a long heat pulse. This may lead to challenges in mass allocation for the systems, though SLA-561V and Acusil-II have been manufactured to similar

[cm]	Acusil-II		SLA-561V		SIRCA-15	
BP	Lift-Up	Lift-Down	Lift-Up	Lift-Down	Lift-Up	Lift-Down
5	1.97	2.43	1.64	1.97	1.14	1.39

Table 10 RSS-sized aftbody TPS thickness (cm) for each trajectory on body point 5.

thicknesses in the past. SLA-561V is installed by hand-packing the composite material into a flexible, honeycomb fiberglass matrix then machining to achieve a smooth outer mold line. The material can be installed on the assembled backshell as has been done for MSL and Mars2020 at nearly the same thickness to the MSL heatshield prior to the change to PICA. Acusil-II was also hand-packed then machined to final thickness for the parachute closeout cone and backshell interface on Mars2020 up to a minimum design thickness of 3.97 cm. On top of having RF-transparency capabilities, Acusil-II satisfies two key needs in covering the backshell. NASA tile systems like SIRCA-15 and AETB-8 are manufacturable to the thickness required but given the size of the backshell, the quantity required would necessarily be in the 100's of tiles which demands high worker-hours to integrate and considerable lot acceptance and configuration management overhead. An option that reduces both the configuration management, and considerable coordination and training of hand-packed materials is a material that could be applied with a spray-gun. The two options known to the authors, SLA-561S and Firex RX 2390 may be applicable, but there is little information available to the author on the thickness achievable along with the scale at which this coating may be applied. Shelf-life limitations may also be of concern as the FireX manufacturer states a shelf-life of 6 months for the compound[22].

VII. Conclusions

As the Ice Giants are NASA's next top-priority destination, it is vital to provide comprehensive and efficient methods to support this mission. Aerocapture has been shown to save both time and fuel to the destination, in turn maximizing the technical payload and shortening the return on investment for the scientific community. The forebody and backshell predicted environments are well within NASA's current ablative TPS capability. The benign backshell environments support a wide range of TPS options. The conventional backshell TPS solutions are sufficient but not optimized for the very low environments predicted, which may incur an unnecessarily high mass and labor cost to implement. Work to develop and demonstrate TPS solutions that can cover large areas with ease while protecting against the entry environments should be undertaken in advance to be ready for vehicle launch in the 2030's. For the forebody, NASA has three viable TPS solutions, with CPICA as the most mass-efficient and advantageous for manufacuturing purposes in this design. While small manufacturing demonstrations on CPICA have shown promise for design-specific bend radius and billets have been produced at size to reduce the number of gaps, investment is required to demonstrate a flight-scale operation with tooling for molded blocks along with sufficient gap-filling for the thickness required. In testing, CPICA has been demonstrated as a gap-filled system in air to relevant environments. Future testing is needed to show there is no risk to the spacecraft for a large-scale, gap-filled heatshield in non-oxidizing environments, though non-oxidative testing in a similar system has shown there is low risk of failure for the system.

References

[1] National Academies of Sciences, E., and Medicine, *Origins, Worlds, and Life: A Decadal Strategy for Planetary Science and Astrobiology 2023-2032*, The National Academies Press, Washington, DC, 2022. https://doi.org/10.17226/26522, URL https://nap.nationalacademies.org/catalog/26522/origins-worlds-and-life-a-decadal-strategy-for-planetary-science.

[2] Dutta, S., Afonso, G., Albert, S. W., Ali, H. K., Allen, G. A., Alunni, A. I., Arnold, J. O., Austin, A., Bailet, G., Bhaskaran, S., et al., "Aerocapture as an Enhancing Option for Ice Giants Missions," 2020.

[3] Deshmukh, R., Dutta, S., Lugo, R., Restrepo, R., Mages, D., Johnson, B., Matz, D., Geiser, J., Scoggins, J., Shellabarger, E., Gomez-Delrio, A., and Williams, J., "Performance Analysis of Aerocapture Systems for Uranus Orbiter," AIAA Paper 2024-XXXX, 2024.

[4] Girija, A. P., "A Flagship-class Uranus Orbiter and Probe mission concept using aerocapture," *Acta Astronautica*, Vol. 202, 2023, pp. 104–118. https://doi.org/https://doi.org/10.1016/j.actaastro.2022.10.005, URL https://www.sciencedirect.com/science/article/pii/S0094576522005422.

[5] Lockwood, M. K., Starr, B. R., Paulson Jr, J. W., Kontinos, D. A., Chen, Y., Laub, B., Olejniczak, J., Wright, M. J., Takashima, N., and Justus, C. G., "Systems analysis for a Venus aerocapture mission," Tech. rep., 2006.

[6] Lockwood, M. K., Edquist, K. T., Starr, B. R., Hollis, B. R., Hrinda, G. A., Bailey, R. W., Hall, J. L., Spilker, T. R., Noca, M. A., and O'Kongo, N., "Aerocapture systems analysis for a Neptune Mission," Tech. rep., 2006.

[7] Spilker, T. R., Adler, M., Arora, N., Beauchamp, P. M., Cutts, J. A., Munk, M. M., Powell, R. W., Braun, R. D., and Wercinski, P. F., "Qualitative Assessment of Aerocapture and Applications to Future Missions," *Journal of Spacecraft and Rockets*, Vol. 56, No. 2, 2019, pp. 536–545. https://doi.org/10.2514/1.A34056, URL https://doi.org/10.2514/1.A34056.

[8] Venkatapathy, E., Prabhu, D., Allen, G., and Gasch, M., "Thermal Protection System to Enable Ice Giant Aerocapture Mission for Delivering both an Orbiter and an In Situ Probe," 2020.

[9] Dutta, S., Shellabarger, E., Scoggins, J., Gomez-Delrio, A., Lugo, R., Deshmukh, R., Chadalavada, P., Williams, J., Garland, J., Johnson, B., Matz, D., Geiser, J., Morgan, J., Restrepo, R., and Mages, J., "Uranus Flagship-class Orbiter and Probe Using Aerocapture," AIAA Paper 2024-XXXX, 2024.

[10] Mages, D., Restrepo, R., Deshmukh, R., Dutta, S., and Benhacine, L., "Mission Design and Navigation Solutions for Uranus Aerocapture," AIAA Paper 2024-XXXX, 2024.

[11] Matz, D., Johnson, B., Geiser, J., Sandoval, S., Deshmukh, R., Lugo, R., Dutta, S., and Chadalavada, P., "Analysis of a Bank Control Guidance for Aerocapture at Uranus," AIAA Paper 2024-XXXX, 2024.

[12] Scoggins, J., Hinkle, A., and Shellabarger, E., "Aeroheating Environment of Aerocapture Systems for Uranus Orbiters," AIAA Paper 2024-XXXX, 2024.

[13] Shellabarger, E., Scoggins, J., Hinkle, A., Dutta, S., Deshmukh, R., Patel, M., and Agam, S., "Aerodynamic Implications of Aerocapture Systems for Uranus Orbiters," AIAA Paper 2024-XXXX, 2024.

[14] Gomez-Delrio, A., and Dutta, S., "Design Implications for Aerocapture Systems Placing Flagship-class Uranus Orbiters," AIAA Paper 2024-XXXX, 2024.

[15] Justh, H., Cianciolo, A. D., Hoffman, J., and Allen Jr, G., "Uranus Global Reference Atmospheric Model (Uranus-GRAM): User Guide," Tech. rep., NASA, 2021.

[16] Brandis, A. M., and Cruden, B. A., *Titan Atmospheric Entry Radiative Heating*, 2017. https://doi.org/10.2514/6.2017-4534, URL https://arc.aiaa.org/doi/abs/10.2514/6.2017-4534.

[17] Mahzari, M., Beck, R., Hwang, H., Monk, J., Morgan, J., Williams, J., and Edquist, K. T., *Development and Sizing of the Mars2020 Thermal Protection System*, ???? https://doi.org/10.2514/6.2022-3951, URL https://arc.aiaa.org/doi/abs/10.2514/6.2022-3951.

[18] Prabhu, D. K., "Exploration of Atmospheric Entries at Saturn, Uranus & Neptune with HEEET as Heatshield TPS," *International Conference on Flight vehicles, Aerothemodynamics and Re-entry Missions (FAR 2019)*, 2019.

[19] Gasch, M., Stackpoole, M., White, S., and Boghozian, T., *Development of Advanced Conformal Ablative TPS Fabricated from Rayon- and Pan-Based Carbon Felts*, ???? https://doi.org/10.2514/6.2016-1414, URL https://arc.aiaa.org/doi/abs/10.2514/6.2016-1414.

[20] Beck, R., Driver, D., Wright, M., Laub, B., Hwang, H., Slimko, E., Edquist, K., Sepka, S., Wilcockson, W., and Thames, T., *Development of the Mars Science Laboratory Heatshield Thermal Protection System*, 2009. https://doi.org/10.2514/6.2009-4229, URL https://arc.aiaa.org/doi/abs/10.2514/6.2009-4229.

[21] Laub, B., and White, S., "Arcjet Screening of Candidate Ablative Thermal Protection Materials for Mars Science Laboratory," *Journal of Spacecraft and Rockets*, Vol. 43, No. 2, 2006, pp. 367–373. https://doi.org/10.2514/1.19218, URL https://doi.org/10.2514/1.19218.

[22] MINTEQ International Inc, "FireX RX 2390 Technical Data Sheet," , 2007. URL https://www.mineralstech.com/docs/default-source/refractories-documents/pyrogenics/firex/firex-rx-2390.pdf?sfvrsn=b11b2c7_0.